AGU PUBLICATIONS

Geophysical Research Letters

RESEARCH LETTER
10.1002/2014GL059275

Key Points:
- Observed ODE frequencies in the Arctic spring have large interannual variability
- The WP pattern is the most significant climate factor for ODE variations
- The influence of the WP pattern on ODEs becomes stronger in the recent decade

Supporting Information:
- Readme
- Figure S1
- Figure S2
- Figure S3
- Figure S4
- Figure S5
- Figure S6

Correspondence to:
Y. Wang,
yuhang.wang@eas.gatech.edu

Citation:
Koo, J.-H., Y. Wang, T. Jiang, Y. Deng, S. J. Oltmans, and S. Solberg (2014), Influence of climate variability on near-surface ozone depletion events in the Arctic spring, *Geophys. Res. Lett.*, *41*, doi:10.1002/2014GL059275.

Received 12 JAN 2014
Accepted 10 MAR 2014
Accepted article online 13 MAR 2014

Influence of climate variability on near-surface ozone depletion events in the Arctic spring

Ja-Ho Koo[1], Yuhang Wang[1], Tianyu Jiang[1], Yi Deng[1], Samuel J. Oltmans[2], and Sverre Solberg[3]

[1]School of Earth and Atmospheric Sciences, Georgia Institute of Technology, Atlanta, Georgia, USA, [2]Earth System Research Laboratory, National Oceanic and Atmospheric Administration, Boulder, Colorado, USA, [3]Norwegian Institute for Air Research (NILU), Kjeller, Norway

Abstract Near-surface ozone depletion events (ODEs) generally occur in the Arctic spring, and the frequency shows large interannual variations. We use surface ozone measurements at Barrow, Alert, and Zeppelinfjellet to analyze if their variations are due to climate variability. In years with frequent ODEs at Barrow and Alert, the western Pacific (WP) teleconnection pattern is usually in its negative phase, during which the Pacific jet is strengthened but the storm track originated over the western Pacific is weakened. Both factors tend to reduce the transport of ozone-rich air mass from midlatitudes to the Arctic, creating a favorable environment for the ODEs. The correlation of ODE frequencies at Zeppelinfjellet with WP indices is higher in the 2000s, reflecting stronger influence of the WP pattern in recent decade to cover ODEs in broader Arctic regions. We find that the WP pattern can be used to diagnose ODE changes and subsequent environmental impacts in the Arctic spring.

1. Introduction

In the Arctic spring, ozone depletion events (ODEs) are often observed near the surface [*Barrie et al.*, 1988; *Simpson et al.*, 2007a]. Recent studies based on satellite and in situ observations suggest that ODEs appear widespread [*Zeng et al.*, 2003, 2006; *Bottenheim et al.*, 2009; *Jacobi et al.*, 2010]. During ODEs, reactive bromine radicals (Br and BrO), produced and recycled by heterogeneous reactions on snow [*Jones et al.*, 2010; *Yang et al.*, 2010], sea ice [*Simpson et al.*, 2007b; *Gilman et al.*, 2010], and aerosol surfaces [*Yang et al.*, 2008; *Frieß et al.*, 2011], not only deplete ozone but also have broad impacts on the Arctic environment. For example, when gas-phase elemental mercury is oxidized by bromine radicals to reactive gaseous mercury and deposited to the Arctic Ocean [*Xie et al.*, 2008], it contributes to atmospheric mercury deposition events (AMDE) [*Steffen et al.*, 2008]. Bromine radicals also oxidize volatile organic compounds [*Keil and Shepson*, 2006] or dimethylsulfide [*von Glasow and Crutzen*, 2004].

The frequency of Arctic ODEs varies greatly from year to year (to be shown in Figure 1). We explore if some of the ODE interannual variability are attributable to climate variation in the Arctic, a region sensitive to climate change [*Solomon et al.*, 2007]. The occurrence and duration of ODEs are a function of bromine activation and recycling [*Simpson et al.*, 2007a; *Liao et al.*, 2012] and air mass transport [*Bottenheim and Chan*, 2006; *Koo et al.*, 2012]. Our current understanding of bromine activation and recycling is too limited to examine how they are affected by climate variability. For example, bromine activation may be enhanced by high wind speed and blowing snow [*Jones et al.*, 2010; *Frieß et al.*, 2011]. However, we do not find a relationship between the interannual variation of ODE frequency and that of the median or 95th percentile wind speed in April. First year sea ice may also enhance bromine activation and recycling [*Simpson et al.*, 2007b], but the large increasing trend of first year sea ice area [*Nghiem et al.*, 2007] does not explain the variation of observed ODE frequencies, which show large interannual variations rather than a clear trend as in the sea ice.

Air mass transport and mixing, on the other hand, are obviously affected by climate factors. Storms over the North Pacific are known to transport ozone-rich air from midlatitudes to the Arctic and are associated with weak ODE occurrence [*Jacobi et al.*, 2010]. We diagnose the variability of regional climate through teleconnection patterns, such as western Pacific (WP) pattern [*Linkin and Nigam*, 2008], Pacific–North American (PNA) pattern [*Leathers and Palecki*, 1992], North Atlantic Oscillation (NAO) [*Hurrell,* 1995], Arctic Oscillation (AO) [*Thompson and Wallace*, 1998], and Pacific Decadal Oscillation (PDO) [*Mantua et al.*, 1997]. Previously, NAO and PNA patterns have been considered as a proxy to diagnose transport of pollutants such as CO [*Eckhardt et al.*, 2003], CO_2 [*Murayama et al.*, 2004], and aerosols [*Di Pierro et al.*, 2011] into the Arctic. The Polar–Eurasian teleconnection

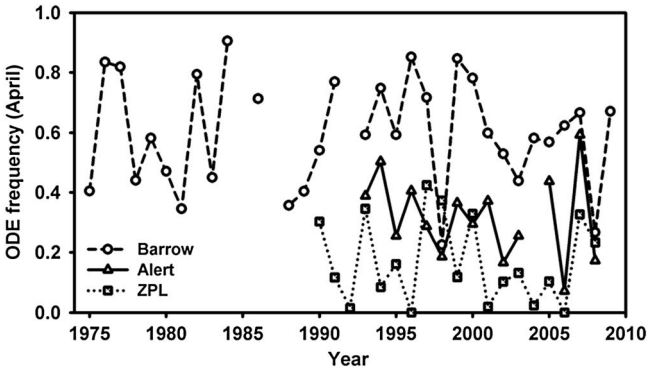

Figure 1. Observed ODE frequencies in April at Barrow, Alert, and ZPL.

patterns appear to influence the trend of AMDEs in the Arctic [*Cole and Steffen*, 2010]. Similarly in this work, we examine how the variability of Arctic spring ODEs relates to regional climate variability. For this purpose, we use long-term ozone measurements made over the past 30 years at three Arctic surface sites.

2. Data and Methods

In this study, we used long-term (at least >15 years) in situ ozone measurements at the three surface sites in the Arctic region, Barrow (71.3°N, 156.8°W; 1980–2009) by the NOAA Earth System Research Laboratory [*Oltmans and levy*, 1994], Alert (82.5°N, 62.3°W; 1993–2008) in the Canadian Air and Precipitation Monitoring Network [*Anlauf et al.*, 1994], and Zeppelinfjellet (ZPL) (78.9°N, 11.9°E; 1990–2008) by the Norwegian Institute for Air Research [*Solberg et al.*, 1996]. Surface ozone concentrations at these sites have been monitored using continuously operating UV absorption systems with an accuracy of 0.5–2 ppbv [*Helmig et al.*, 2007]. Ozonesonde data are not used because they are too limited in providing useful information on the interannual variation of ODE frequency in April.

To investigate the influence of regional climate variability on the Arctic ODEs, we used five monthly teleconnection indices including WP, PNA, NAO, AO, and PDO. Rotated principal component analysis [*Wallace and Gutzler*, 1981] was used to calculate the monthly indices of WP, PNA, and NAO, and empirical orthogonal functions applied to the monthly mean 1000 hPa height anomaly poleward of 20°N in the northern hemisphere were used to compute a monthly AO index [*Thompson and Wallace*, 1998]. The PDO index was obtained from the leading principal component of monthly sea surface temperature variability in the North Pacific poleward of 20°N [*Mantua et al.*, 1997]. All climate variability indices used in this study except PDO were obtained from the NOAA Climate Prediction Center (http://www.cpc.ncep.noaa.gov/data/teledoc/telecontents.shtml). The PDO index was obtained from the Joint Institute for the Study of the Atmosphere and Ocean at the University of Washington (http://jisao.washington.edu/pdo/).

In addition to the regional climate indices, we also examined large-scale dynamics using the National Centers for Environmental Prediction/National Center for Atmospheric Research (NCEP/NCAR) Reanalysis data [*Kalnay et al.*, 1996], which are obtained from the NOAA web site (http://www.esrl.noaa.gov/psd/data/gridded/reanalysis/). The jet stream across the Pacific was diagnosed using 300 hPa winds. The Pacific storm track was diagnosed by tracking the low-pressure centers at sea level every 6 h based on an algorithm developed by *Hoskins and Hodges* [2002]. The tracking results were regridded onto regular grids (2.5° × 2.5°) by considering both the intensity and distance of the tracked cyclones around a given grid point [*Cressman*, 1959]. By removing the climatology mean of the storm track intensity, we obtained the anomaly of storm track intensity. The procedure adopted here to obtain the intensity of the storm track is widely used for the analysis of regional cyclonic activity [*Myoung and Deng*, 2009]. Similar results (not shown) are obtained by examining the distribution of storm track occurrence density. Based on the NCEP/NCAR Reanalysis data, the anomaly of sea level pressure (SLP) was also estimated using the 30 year climatology (1981–2010).

3. Results and Discussion

Here we use the normalized ODE frequency in April, which is defined as the ratio of the hours of ozone mixing ratio <10 ppbv to the total observation hours in a month [*Oltmans et al.*, 2012]. The normalized ODE frequency is a good indicator to show the range of monthly mean ozone concentration (Figure S1a in the supporting information). The time series and histograms of ODE frequencies in April at Barrow, Alaska (71.3°N, 156.8°W), Alert, Canada (82.5°N, 62.3°W), and Zeppelinfjellet, Norway (78.9°N, 11.9°E) are compared (Figure 1 and Figure S1b in the supporting information). The ODE frequency is usually highest at Barrow and lowest at ZPL due in part to the altitude of the observatory (474 m). The most striking feature at all the sites is the large interannual variability. A high-ODE year is sometimes followed by a low-ODE year.

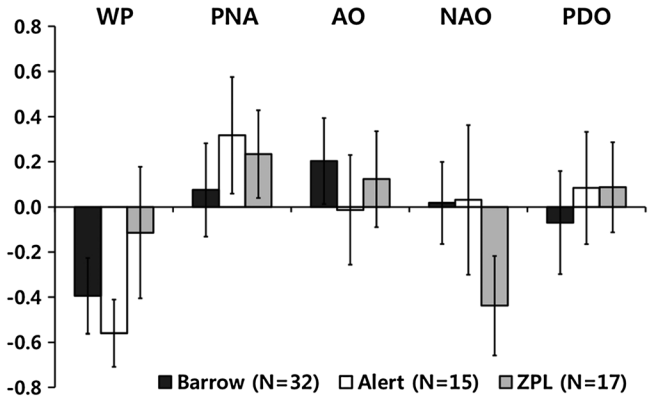

Figure 2. Spearman's Rank correlation coefficients (ρ) of ODE frequencies at the three monitoring sites with five teleconnection indices in the northern hemisphere, including western Pacific pattern, Pacific–North American pattern, Arctic Oscillation, North Atlantic Oscillation, and Pacific Decadal Oscillation. Vertical bars indicate the 1σ uncertainties estimated with 20,000 bootstraps. The number of years of available ozone measurements at each site is shown in the parentheses.

To explore the relationship between interannual variation of ODEs and large-scale climatic patterns, we compute the nonparametric Spearman's rank correlation coefficients (ρ) of ODE frequencies at the three sites with five indices of climate variability: WP, PNA, AO, NAO, and PDO (Figure 2). Bootstrap (20,000 times) is used to estimate the uncertainties. Very similar results are obtained using Pearson's correlation coefficient. The three most significant correlations are between the WP index and ODE frequencies at Barrow and Alert, respectively, and between the NAO index and ODE frequency at ZPL. We will show later that a smaller correlation with the WP index at ZPL is due to a decadal change in the effect of WP on ZPL ODEs (to be shown in Figure 5). In the 2000s, all three sites show consistent negative correlations between ODE frequency and the WP index. We do not find another climate index that has such consistency across the three sites.

Similar results are obtained by examining the average index values for strong ODE years in comparison to weak ODE years (Figure S2 in the supporting information). We selected 5 years with the most frequent ODEs and 5 years with the least frequent ODEs, respectively, at each site in this analysis. Strong ODE years have a negative average WP index, and weak ODE years have a positive average WP index at Barrow and Alert. The index phase changes for the other teleconnection patterns between strong and weak ODE years are not as drastic at these two sites. We also compare the anomalies of sea level pressure for strong and weak ODE years at Barrow and Alert with those for positive and negative WP index years (Figure S3 in the supporting information). The SLP anomalies in weak ODE years clearly differ from strong ODE years. The distribution pattern of the former (latter) is much closer to the SLP anomaly distribution in positive (negative) WP index years.

As discussed previously, atmospheric transport can strongly affect ODEs in the Arctic. In the northern hemisphere, the WP pattern is associated with the variability of jet stream and storm track in the Pacific [*Lau,* 1988; *Linkin and Nigam,* 2008]. The cross Pacific jet stream is zonally extended much farther toward North America in the negative than in the positive phase of the WP pattern; more anticyclonic (cyclonic) wave breaking during the positive (negative) WP pattern favors to the more northern (southern) location of the jet stream [*Rivière,* 2010]. The changing jet stream (30–40°N) pattern further affects the intensity of the northern Pacific storm track (50–60°N) [*Lee et al.*, 2010; *Penny et al.*, 2013]. These dynamic modulations associated with the WP pattern appear to be related to Rossby wave breaking [*Rivière,* 2010] and meridional temperature gradient change over the western Pacific [*Lee et al.*, 2010].

Since the chemical production of ozone is very slow in spring [*Wang et al.*, 2003], ODEs are mainly terminated by mixing with ozone-rich air. Previously, migration of low-pressure systems from midlatitudes to the Arctic was found to cause termination of Arctic ODEs [*Jacobi et al.*, 2010] due in part to the transport of ozone-rich air masses by storms. Atmospheric mixing is also important in ODE formation because the Arctic ODEs are usually observed in a thermally stable atmosphere, which reduces mixing with ozone-rich free tropospheric air [*Zeng et al.*, 2006; *Koo et al.*, 2012]. The vertical mixing caused by storms mixes low-ozone with high-ozone air and terminates ODEs.

The hypothesis that we test here is if the negative WP phase is associated with jet stream and storm track conditions that favor ODEs in the Arctic. At Barrow and Alert, the Pacific jet stream extends much closer to North America in strong ODE years than in weak ODE years (Figure 3). A strong jet stream acts as a barrier of meridional mixing between midlatitudes and the Arctic. More evidence are found in the change of the

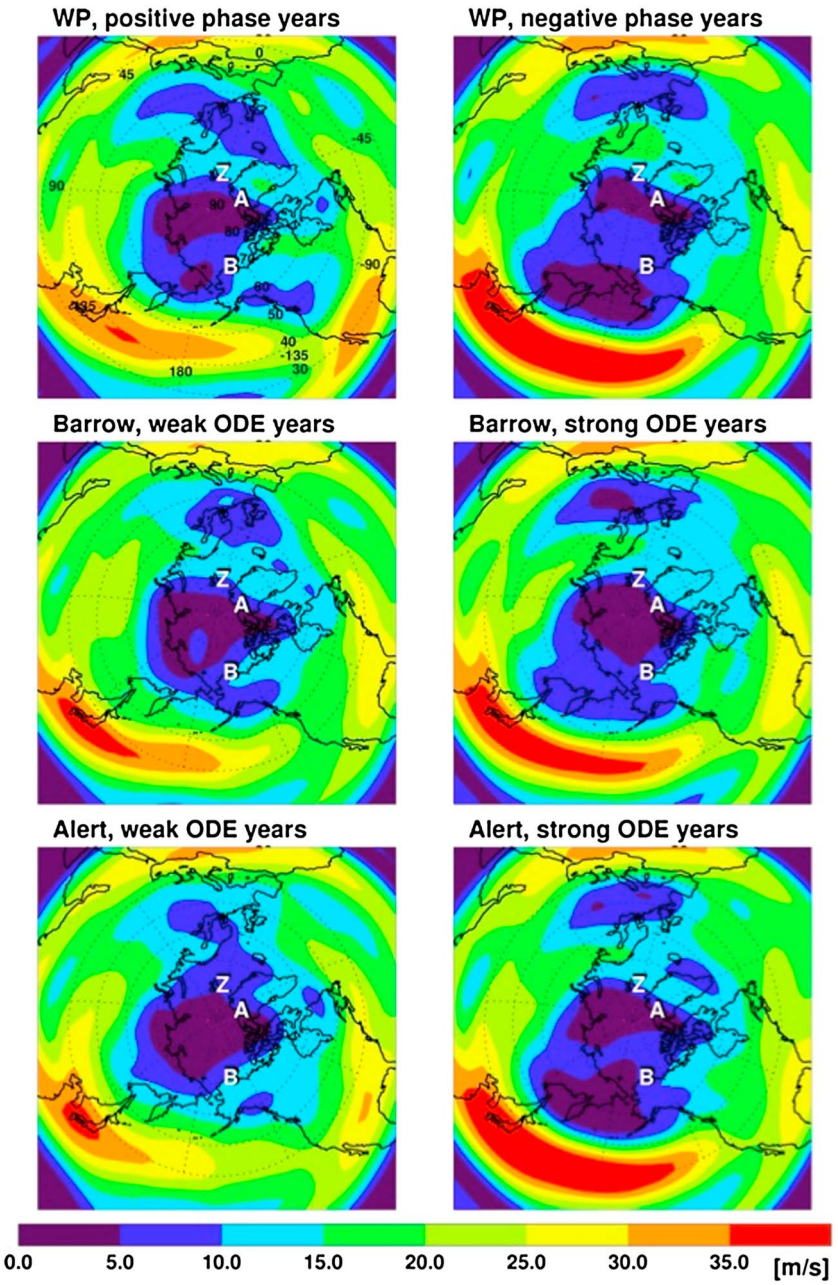

Figure 3. Composite images of 300 hPa wind speed in (top) the northern hemisphere during the positive and negative phase years of WP pattern and weak and strong ODE years at (middle) Barrow and (bottom) Alert. For each case, five most extreme years are selected and averaged. The locations of Barrow, Alert, and ZPL are marked B, A, and Z, respectively. The unit of color bar is m/s.

Pacific storm track that extends from East Asia through the Bering Sea toward Barrow. It is weaker in strong ODE years than in weak ODE years (Figure 4 and Figure S4 in the supporting information). A weak storm track leads to reduced air mass transport to the Arctic and vertical mixing between boundary layer and free tropospheric ozone. Both a strong jet and a weak storm track over the Pacific are inductive to ODE occurrence in the Arctic, resulting in the negative correlation between ODE frequency and WP index (Figure 2 and Figure S2 in the supporting information). In contrast, the intensity of the Atlantic storm track does not show a large difference between strong and weak ODE years at Barrow and Alert (Figure 4), implying that these sites are not affected significantly by Atlantic storms.

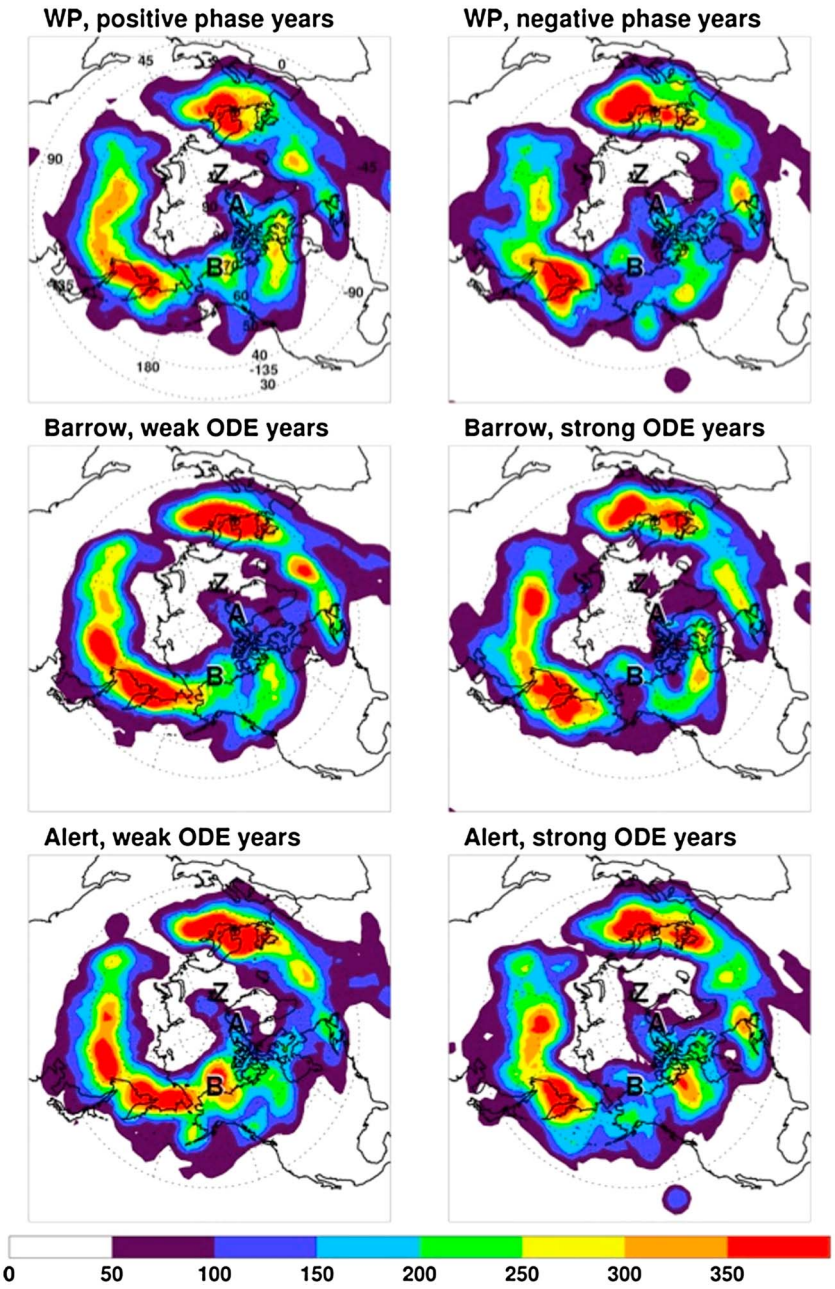

Figure 4. Same as Figure 3 but for composite images of storm track intensity in the northern hemisphere. The unit of color bar is pascal.

ZPL is situated much farther away from the Pacific compared to Barrow and Alert. It is therefore not surprising that we found a weaker correlation between WP index and ODE occurrence at this site. Figure S5 in the supporting information shows that neither the zonal extension of the Pacific jet stream nor storm track intensities indicate as clear a difference between strong and weak ODE years of ZPL as at Barrow or Alert (Figures 3 and 4).

However, further analysis reveals an interesting shift of WP influence on ZPL from 1990s to 2000s. Comparing the ozone measurements among the three sites shows a clear decadal scale change in the correlations of ZPL ODE frequency with the other two sites. Figure 5a shows that ODE frequencies are positively correlated between Barrow and Alert in the 1990s (1990–1999) and 2000s (2000–2009). In contrast, the ZPL ODE

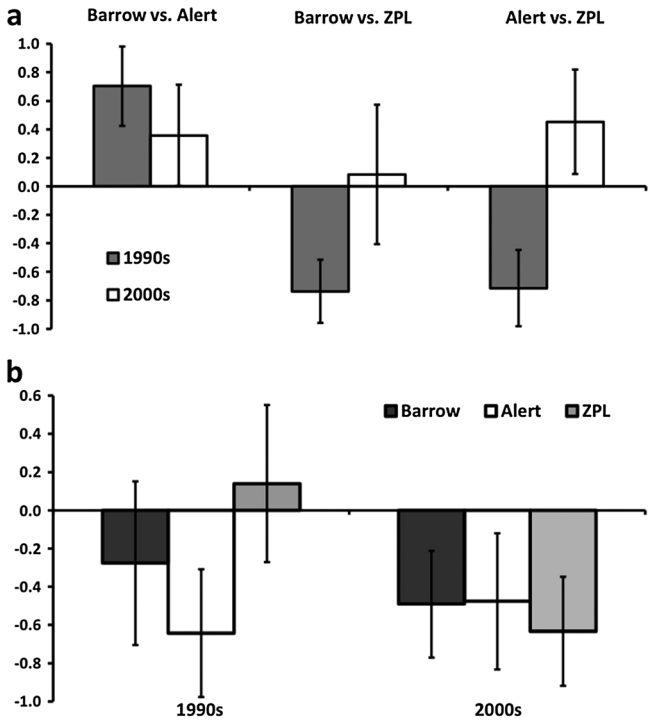

Figure 5. (a) Rank correlation coefficients (ρ) of ODE frequency among Barrow, Alert, and ZPL in 1990s (gray) and 2000s (white). (b) Rank correlation coefficients of the WP index with ODE frequency at the three sites in 1990s and 2000s. Vertical bars show 1σ uncertainties estimated with 20,000 bootstraps.

frequency has negative correlations with the other two sites in the 1990s but switches to a neutral or positive correlation in the 2000s. Figure 5b shows negative correlations between the WP index and ODE frequency at Barrow or Alert in the 1990s and 2000s, although the correlation at Barrow is weak in 1990s. While the ODE frequency at ZPL has a small and insignificant positive correlation with the WP index in the 1990s, the correlation turns largely negative in the 2000s. In fact, the three sites have consistently negative correlations between the WP index and ODE frequency in the 2000s.

We then examine the storm track distributions in strong and weak ZPL ODE years separately in the 1990s and 2000s (Figure S6a in the supporting information). In the 1990s, the storm track originating in the Pacific did not reach ZPL. In the 2000s, the Pacific storm track activities were more intense near ZPL in weak ODE years than strong ODE years. This is consistent with the finding in Figure 4 that a strong Pacific storm track enhances the atmospheric mixing and the transport of ozone-rich air masses from lower latitudes, leading to a lower ODE frequency.

More insight into the atmospheric condition is found in the anomaly of SLP in the 1990s and 2000s (Figure S6b in the supporting information). The SLP anomalies appear to be similar in strong ZPL ODE years in the 1990s and 2000s, characterized by a low-pressure anomaly over the Kara-Barent Sea, where satellite observations indicated high BrO columns [*Zeng et al.*, 2003, 2006; *Koo et al.*, 2012]. During the weak ODE years when we expected more mixing with lower latitude ozone-rich air masses, the SLP anomaly in the 1990s is different from the 2000s. The average SLP anomaly of the 1990s is similar to the negative phase of the AO. The average SLP anomaly of the 2000s in weak ZPL ODE years, on the other hand, is similar to the positive phase of WP pattern, reflecting the effect of WP pattern on ODEs at ZPL (Figure 5).

4. Conclusions

We study in this work the impacts of regional climate variability on near-surface ODE frequencies at Barrow, Alert, and ZPL in the past 3 decades. Barrow and Alert tend to have higher ODE frequencies in the negative than in the positive phase of the WP pattern, when a stronger Pacific jet stream and less intense storm track activities lead to less lateral and vertical mixing with ozone-rich air. The influence of the WP pattern at ZPL is stronger in the 2000s than in the 1990s. The high Arctic appears to be influenced more strongly by the WP pattern in the 2000s than in the 1990s. The reason is unclear. One possibility is the high sensitivity of Arctic climate to aerosol loadings over East Asia, which has been increasing rapidly in 2000s [*Levy et al.*, 2008; *Streets et al.*, 2013]. Another possibility is the global climate change in the recent decade [*Solomon et al.*, 2007]. Tropical climate variability, such as the El Niño–Southern Oscillation, can also affect the WP pattern [*Yeh and Kirtman*, 2004], through which ODEs in the Arctic spring can be influenced. Further studies are needed to evaluate these mechanisms. We find that the chemical environment of the Arctic, including ODEs and consequently atmospheric mercury deposition, is sensitive to regional climate variability. The results

presented here suggest that the long-term change of WP pattern is a key factor in understanding and projecting potential impacts of future global climate changes on the Arctic chemical environment in spring.

Acknowledgments
This work was supported by the NASA International Polar Year and Atmospheric Chemistry Modeling and Analysis Programs. The ozone data at Alert were provided by Mike Shaw and Dave Ord of Environment Canada, and the ozone data at ZPL were provided by Ann Mari Fjaeraa of NILU.

The Editor thanks two anonymous reviewers for their assistance in evaluating this paper.

References

Anlauf, K. G., R. E. Mickle, and N. B. A. Trivett (1994), Measurement of ozone during Polar Sunrise Experiment 1992, *J. Geophys. Res.*, *99*, 25,345–25,353.

Barrie, L. A., J. W. Bottenheim, R. C. Schnell, P. J. Crutzen, and R. A. Rasmussen (1988), Ozone destruction and photochemical reactions at polar sunrise in the lower Arctic atmosphere, *Nature*, *334*, 138–141.

Bottenheim, J. W., and E. Chan (2006), A trajectory study into the origin of spring time Arctic boundary layer ozone depletion, *J. Geophys. Res.*, *111*, D19301, doi:10.1029/2006JD007055.

Bottenheim, J. W., S. Netcheva, S. Morin, and S. V. Nghiem (2009), Ozone in the boundary layer air over the Arctic Ocean: Measurements during the TARA transpolar drift 2006–2008, *Atmos. Chem. Phys.*, *9*, 4545–4557.

Cole, A. S., and A. Steffen (2010), Trends in long-term gaseous mercury observations in the Arctic and effects of temperature and other atmospheric conditions, *Atmos. Chem. Phys.*, *10*, 4661–4672.

Cressman, G. P. (1959), An operational objective analysis system, *Mon. Weather Rev.*, *87*, 367–374.

Di Pierro, M., L. Jaeglé, and T. L. Anderson (2011), Satellite observations of aerosol transport from East Asia to the Arctic: Three case studies, *Atmos. Chem. Phys.*, *11*, 2225–2243.

Eckhardt, S., A. Stohl, S. Beirle, N. Spichtinger, P. James, C. Forster, C. Junker, T. Wagner, U. Platt, and S. G. Jennings (2003), The North Atlantic Oscillation controls air pollution transport to the Arctic, *Atmos. Chem. Phys.*, *3*, 1769–1778.

Frieß, U., H. Sihler, R. Sander, D. Pöhler, S. Yilmaz, and U. Platt (2011), The vertical distribution of BrO and aerosols in the Arctic: Measurements by active and passive differential optical absorption spectroscopy, *J. Geophys. Res.*, *116*, D00R04, doi:10.1029/2011JD015938.

Gilman, J. B., et al. (2010), Ozone variability and halogen oxidation within the Arctic and sub-Arctic springtime boundary layer, *Atmos. Chem. Phys.*, *10*, 10,223–10,236.

Helmig, D., S. J. Oltmans, D. Carlson, J.-F. Lamarque, A. Jones, C. Labuschagne, K. Anlauf, and K. Hayden (2007), A review of surface ozone in the polar regions, *Atmos. Environ.*, *41*, 5138–5161.

Hoskins, B. J., and K. I. Hodges (2002), New perspectives on the Northern Hemisphere winter storm tracks, *J. Atmos. Sci.*, *59*, 1041–1061.

Hurrell, J. W. (1995), Decadal trends in the North Atlantic Oscillation and relationships to regional temperature and precipitation, *Science*, *269*, 676–679.

Jacobi, H.-W., S. Morin, and J. W. Bottenheim (2010), Observation of widespread depletion of ozone in the springtime boundary layer of the central Arctic linked to mesoscale synoptic conditions, *J. Geophys. Res.*, *115*, D17302, doi:10.1029/2010JD013940.

Jones, A. E., P. S. Anderson, E. W. Wolff, H. K. Roscoe, G. J. Marshall, A. Richter, N. Brough, and S. R. Colwell (2010), Vertical structure of Antarctic tropospheric ozone depletion events: Characteristics and broader implications, *Atmos. Chem. Phys.*, *10*, 7775–7794.

Kalnay, E., et al. (1996), The NCEP/NCAR 40-year reanalysis project, *Bull. Am. Meteorol. Soc.*, *77*, 437–471.

Keil A. D., and P. B. Shepson (2006), Chlorine and bromine atom ratios in the springtime Arctic troposphere as determined from measurements of halogenated volatile organic compounds, *J. Geophys. Res.*, *111*, D17303, doi:10.1029/2006JD007119.

Koo, J.-H., et al. (2012), Characteristics of tropospheric ozone depletion events in the Arctic spring: Analysis of the ARCTAS, ARCPAC, and ARCIONS measurements and satellite BrO observations, *Atmos. Chem. Phys.*, *12*, 9909–9922.

Lau, N.-C. (1988), Variability of the observed midlatitude storm tracks in relation to low-frequency changes un the circulation pattern, *J. Atmos. Sci.*, *45*, 2718–2743.

Leathers, D. J., and M. A. Palecki (1992), The Pacific/North American teleconnection pattern and United States climate II: Temporal characteristics and index specification, *J. Clim.*, *5*, 707–716.

Lee, Y. Y., G.-H. Lim, and J.-S. Kug (2010), Influence of the East Asian winter monsoon on the storm track activity over the North Pacific, *J. Geophys. Res.*, *115*, D09102, doi:10.1029/2009JD012813.

Levy, H., II, M. D. Schwarzkopf, L. Horowitz, V. Ramaswamy, and K. L. Findell (2008), Strong sensitivity of late 21st century climate to projected changes in short-lived air pollutants, *J. Geophys. Res.*, *113*, D06102, doi:10.1029/2007JD009176.

Liao, J., et al. (2012), Characterization of soluble bromide measurements and a case study of BrO observations during ARCTAS, *Atmos. Chem. Phys.*, *12*, 1327–1338.

Linkin, M. E., and S. Nigam (2008), The north Pacific oscillation-west Pacific teleconnection pattern: Mature-phase structure and winter impacts, *J. Clim.*, *21*, 1979–1997.

Mantua, N. J., S. R. Hare, Y. Zhang, J. M. Wallace, and R. C. Francis (1997), A Pacific interdecadal climate oscillation with impacts on salmon production, *Bull. Am. Meteorol. Soc.*, *78*, 1069–1079.

Murayama, S., S. Taguchi, and K. Higuchi (2004), Interannual variation in the atmospheric CO_2 growth rate: Role of atmospheric transport in the northern hemisphere, *J. Geophys. Res.*, *109*, D02305, doi:10.1029/2003JD003729.

Myoung, B., and Y. Deng (2009), Interannual variability of the cyclonic activity along the U.S. Pacific coast: Influences on the characteristics of winter precipitation in the western United States, *J. Clim.*, *22*, 5732–5747.

Nghiem, S. V., I. G. Rigor, D. K. Perovich, P. Clemente-Colo´n, J. W. Weatherly, and G. Neumann (2007), Rapid reduction of Arctic perennial sea ice, *Geophys. Res. Lett.*, *34*, L19504, doi:10.1029/2007GL031138.

Oltmans, S. J., and H. Levy II (1994), Surface ozone measurements from a global network, *Atmos. Environ.*, *28*, 9–24.

Oltmans, S. J., B. J. Johnson, and J. M. Harris (2012), Springtime boundary layer ozone depletion at Barrow, Alaska: Meteorological influence, year to year variation, and long-term change, *J. Geophys. Res.*, *117*, D00R18, doi:10.1029/2011JD016889.

Penny, S. M., D. S. Battisti, and G. H. Roe (2013), Examining mechanisms of variability within the Pacific storm track: Upstream seeding and jet-core strength, *J. Clim.*, *26*, 5242–5259.

Rivière, G. (2010), Role of Rossby wave breaking in the west Pacific teleconnection, *Geophys. Res. Lett.*, *37*, L11802, doi:10.1029/GL043309.

Simpson, W. R., et al. (2007a), Halogens and their role in polar boundary-layer ozone depletion, *Atmos. Chem. Phys.*, *7*, 4375–4418.

Simpson, W. R., D. Carlson, G. Hönninger, T. A. Douglas, M. Sturn, D. Perovich, and U. Platt (2007b), First-year sea-ice contact predicts bromine monoxide (BrO) levels at Barrow, Alaska better than potential frost flower contact, *Atmos. Chem. Phys.*, *7*, 621–627.

Solberg, S., N. Schmidbauer, A. Semb, and F. Stordal (1996), Boundary layer ozone depletion as seen in the Norwegian Arctic in spring, *J. Atmos. Chem.*, *23*, 301–332.

Solomon, S., D. Qin, M. Manning, Z. Chen, M. Marquis, K. Averyt, M. Tignor, and H. Miller (Eds.) (2007), *Climate Change 2007: The Physical Science Basis. Contribution of Working Group I to the Fourth Assessment Report of the Intergovernmental Panel on Climate Change*, Cambridge Univ. Press, Cambridge, U. K.

Steffen, A., et al. (2008), A synthesis of atmospheric mercury depletion event chemistry in the atmosphere and snow, *Atmos. Chem. Phys.*, *8*, 1445–1482.

Streets, D. G., D. T. Shindell, Z. Lu, and G. Faluvegi (2013), Radiative forcing due to major aerosol emitting sectors in China and India, *Geophys. Res. Lett.*, *40*, 4409–4414, doi:10.1002/grl.50805.

Thompson, D. W. J., and J. M. Wallace (1998), The Arctic oscillation signature in the wintertime geopotential height and temperature fields, *Geophys. Res. Lett.*, *25*, 1297–1300.

von Glasow, R., and P. J. Crutzen (2004), Model study of multiphase DMS oxidation with a focus on halogens, *Atmos. Chem. Phys.*, *4*, 589–608.

Wallace, J. M., and D. S. Gutzler (1981), Teleconnections in the geopotential height field during the Northern Hemisphere winter, *Mon. Weather Rev.*, *109*, 784–812.

Wang, Y., et al. (2003), Springtime photochemistry at northern mid and high latitudes, *J. Geophys. Res.*, *108*(D4), 8358, doi:10.1029/2002JD002227.

Xie, Z. Q., R. Sander, U. Pöschl, and F. Slemr (2008), Simulation of atmospheric mercury depletion events (AMDEs) during polar springtime using the MECCA box model, *Atmos. Chem. Phys.*, *8*, 7165–7180.

Yang X., J. A. Pyle, and R. A. Cox (2008), Sea salt production and bromine release: Role of snow on sea ice, *Geophys. Res. Lett.*, *35*, L16815, doi:10.1029/2008GL034536.

Yang, X., J. A. Pyle, R. Q. Cox, N. Theys, and M. Van Roozendael (2010), Snow-sourced bromine and its implications for polar tropospheric ozone, *Atmos. Chem. Phys.*, *10*, 7763–7773.

Yeh, S.-W., and B. P. Kirtman (2004), The North Pacific Oscillation-ENSO and internal atmospheric variability, *Geophys. Res. Lett.*, *31*, L13206, doi:10.1029/2004GL019983.

Zeng, T., Y. Wang, K. Chance, E. V. Browell, B. A. Ridley, and E. L. Atlas (2003), Widespread persistent near-surface ozone depletion at northern high latitudes in spring, *Geophys. Res. Lett.*, *30*(24), 2298, doi:10.1029/2003GL018587.

Zeng, T., Y. Wang, K. Chance, N. Blake, D. Blake, and B. Ridley (2006), Halogen-driven low-altitude O3 and hydrocarbon losses in spring at northern high latitudes, *J. Geophys. Res.*, *111*, D17313, doi:10.1029/2005JD006706.